Fade Countermeasure using Signal Degradation Estimation for Demand-Assignment Satellite Systems

Nedo Celandroni, Francesco Potortì

Abstract:This paper describes a complete fade countermeasure system, designed for thin route user-oriented and fully meshed satellite networks. The signal degradation due to the residual up-link attenuation after up-power control intervention, plus the down-link attenuation, is compensated for by varying the FEC coding and bit rates of the data. Down and up-link signal degradations are evaluated separately: the former by collecting statistics of quantised levels of the demodulated PSK signal, and the latter by using a narrow band signal level estimator. Measurement times are optimised using a model to evaluate the scintillation variance. The performance evaluation of the whole system in the presence of additive white Gaussian noise (AWGN), shows that very small link power margins can be adopted.

Index Terms:Fade countermeasure, Scintillation, FEC, Signal quality estimation, Power margin

I. INTRODUCTION

Using the Ka band for satellite communications entails solving the rain fading problem to ensure an acceptable availability of the link. The fade countermeasure system we present, which was developed as a prototype and used for an experiment on the Olympus and Italsat satellites [4], is cost effective compared to others such as space [10] or frequency diversity [12, 13, 21] and very efficient in the case of low-medium fade intensity. Our system is based on the adaptation of the energy per information bit to the channel fading conditions in order to maintain the quality of data within the requirements specified by the user. The total attenuation of each link (up-link plus down-link) is compensated for by varying the transmission power first, then FEC coding and bit rates when necessary. A multicarrier access to the satellite transponder is envisaged to exploit the entire transponder bandwidth with limited data rates of each carrier, thus the modest performance required by the earth stations allows the antennas to be installed on the user's premises. The transmission power variation must ensure a constant back-off at the transponder input in order to control the intermodulation noise. The power control can thus be used to compensate for up-link attenuations only, while the total compensation is completed by varying the FEC coding and bit rates as well.

A key requirement in fade countermeasure systems is the need to detect the signal quality quickly and accurately. This paper describes a fade countermeasure system using both a signal quality and an attenuation estimator. It presents a performance evaluation of the system in the presence of additive white Gaussian noise (AWGN), and gives numerical results in terms of link budget margin. The performance of the estimators is studied by using a scintillation model derived from experimental data. The signal quality estimator is based on the statistics of quantised levels of PSK demodulated signals which are also used for Viterbi decoders, while a narrow band signal level estimator is employed to evaluate the up-link attenuation.

We consider a user-oriented demand assignment-time division multiple access (DA-TDMA) channel access scheme, suitable for supporting both real-time (telephony and video) and non real-time (computer data exchange) application traffic on a fully meshed network topology. The system, named FIFO Ordered Demand Assignment/Information Bit Energy Adaptive (FODA/IBEA) [2-4], was developed and tested on the Italsat satellite. It is based on a centralised control of the channel capacity assignment algorithm according to user demand. Each traffic station is able to send/receive data to/from all the other stations, while a master station is responsible for both system synchronisation and the capacity allocation on demand of the traffic stations (see Fig. 1). To accomplish its task the master sends a reference burst (RB) which contains the transmission times of the traffic stations (allocations) for both real-time and non real-time traffic. The RB is sent at the beginning of each 20 ms frame. The traffic stations receive the allocations two round trip times after sending their requests. We assume for the sake of simplicity that each active station transmits one data burst per frame containing control information plus any number of data packets. The burst control information contains per-packet addresses, FEC coding and bit rates. Each station measures the receiving power of the RB and uses it as a reference level, tracking it by varying the transmission power of its own data bursts. This way the up-link attenuation is compensated for in the power range of the up-link power control. Any up-link excess attenuation adds to the total degradation of the signal in addition to the attenuation on the receiving station down-link. Due to the delay between the request and the allocation of the bandwidth, an accurate evaluation of the time variance of the signal degradation is needed to reduce the link power margin. Using the scintillation model developed in [1] we optimise both the signal quality and the signal level estimations in order to minimize the power margin.

Although the fade countermeasure system presented is rather specific in terms of the hardware employed, most of the

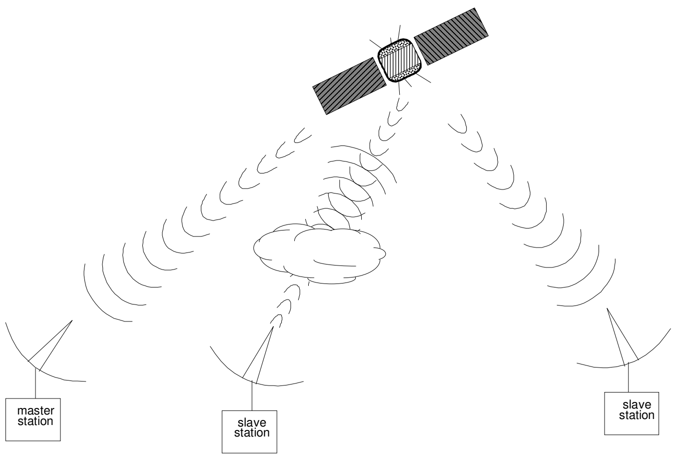

Fig 1. One master and two traffic stations, one of which is in fading conditions

techniques used and results obtained are of a more general validity.

In Section II the signal quality estimator is presented. The results of the scintillation model developed in [1] are used in Section III to estimate both the signal quality and the up-link attenuation variances. Measurement time intervals are optimised in Section IV, and the performance of the overall system is shown in Section V. Conclusions are drawn in Section VI.

II. SIGNAL QUALITY ESTIMATOR

The signal quality estimator that we are going to describe is a weighted average of the soft levels of the demodulated bits. Hereafter we assume that binary PSK is being used, although extending QPSK is straightforward.

Fig. 2 illustrates the functional block diagram of the digital communication system considered, where a convolutional encoder and a Viterbi decoder are employed.

Soft decisions are preferred to hard decisions because of their higher coding gain. Our estimator uses the soft levels employed by the decoder, thus requiring very little additional hardware.

The output of the PSK demodulator (matched filter receiver) sampled at the instant t_k can be expressed as

$$o_k = \pm\sqrt{E_b} + n_k,$$

where the plus or minus sign is selected depending on whether the transmitted bit is a 1 or a 0 [20].

The random variable n_k represents the AWGN at the sampling instant t_k with zero mean and $N_o/2$ variance (N_o is the one-sided noise power density), while E_b is the energy per bit of the transmitted signal.

The demodulated analog signal is converted into digital data y_i ($i = 1, 2, \ldots, Q$) at the A/D converter based on the soft decision thresholds $b_1, b_2, \ldots, b_{Q-1}$, as shown in Fig. 3.

By using the conditional probability that the signal received falls into a generic quantisation interval regardless of the value (0 or 1) of the transmitted bit, we can write the probability for each quantisation level i as:

$$P_i(R) = \frac{1}{2}\left\{ \begin{array}{l} \operatorname{erfc}\left[10^{R/20}(1-h_i)\right] - \operatorname{erfc}\left[10^{R/20}(1-h_{i-1})\right] + \\ + \operatorname{erfc}\left[10^{R/20}(1+h_{i-1})\right] - \operatorname{erfc}\left[10^{R/20}(1+h_i)\right] \end{array} \right\} \quad (1)$$

where:

$$h_i = \begin{cases} \dfrac{i}{Q/2} & i = 0, \ldots, Q/2-1 \\ +\infty & i = Q/2 \end{cases},$$

R is the E_b/N_o ratio expressed in dB and

$$\operatorname{erfc}(x) \stackrel{\Delta}{=} \frac{2}{\sqrt{\pi}} \int_x^{\infty} e^{-t^2}\, dt .$$

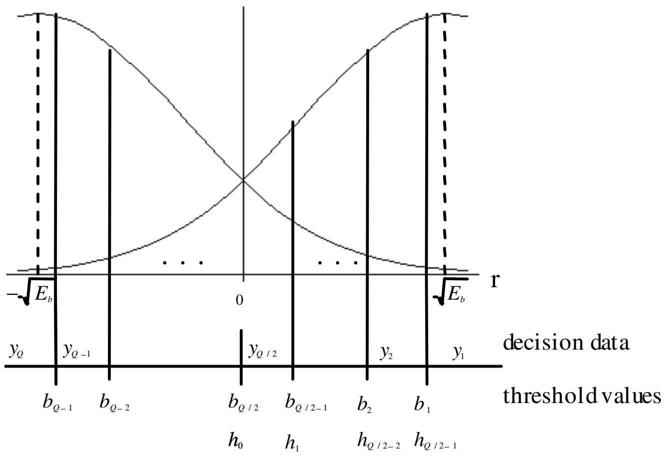

Fig 3. Conditional probability density functions of the signal and soft decision levels

We call *quality* the random variable q that associates a weight q_i with each quantisation level. The mean of this random variable is a monotonic function of the E_b/N_o value of the signal received, so it can be used as an estimator of E_b/N_o. We can evaluate the mean and the variance of q as:

$$\mu_q(R) = \sum_1^{Q/2} q_i P_i(R), \quad \sigma_q^2(R) = \sum_1^{Q/2} q_i^2 P_i(R) - \mu_q^2(R).$$

Let us denote by $\bar{q}$ the sample mean of q over a large number of received bits N. For the central limit theorem [7], the distribution of $\bar{q}$ is well approximated by a normal distribution with mean

$$\mu_{\bar{q}}(R) = \mu_q(R)$$

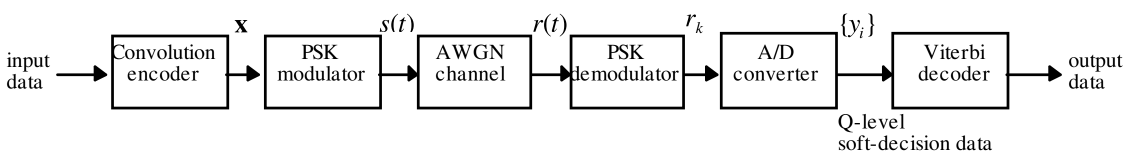

Fig 2. The channel model considered for the signal quality estimator

and variance

$$\sigma_{\bar{q}}^2(R) = \sigma_q^2(R)/N .$$

The function $\mu_{\bar{q}}(R)$ is monotonic for suitable values of q_i, so it can be inverted and for each $\bar{q}$, we can find an estimation of R denoted by $\hat{R}(\bar{q})$. For sufficiently small $\sigma_{\bar{q}}^2(R)$, the distribution of $\hat{R}$ can be considered as being normal as well, with an upper-bounded variance given by

$$\sigma_{\hat{R}}^2(R) = \frac{\sigma_q^2(R)}{\left(\Delta\mu_q(R)/\Delta R\right)^2 N}, \qquad (2)$$

where

$$\Delta\mu_q/\Delta R = \min\left\{\left[\Delta\mu_q/\Delta R\right]^+, \left[\Delta\mu_q/\Delta R\right]^-\right\}$$

($[\cdot]^+$ and $[\cdot]^-$ are the right and left incremental ratios, respectively, and $\Delta\mu_q = 3\sigma_{\bar{q}}$). In [5] a similar case is analysed and the approximation error of relation (2) is given.

There are many degrees of freedom for choosing the weights even with the constraint that $\mu_{\bar{q}}(R)$ be monotonic, so it is possible to choose them in order to minimise $\sigma_{\hat{R}}^2(R)$ over the operating range of R, which means minimising the estimation error. Once this minimisation has been done, the mean of the quality can be used as the argument of $\hat{R}(\bar{q})$, which is what we call the *quality estimator* of the E_b/N_o ratio.

A. Practical Implementation

We used a modem with equally spaced soft decision thresholds, which is a near optimum choice for a Viterbi decoder [8]. We minimised the variance of $\hat{R}$ by simply minimising the sum of the variances of $\hat{R}$ taken at the borders and in the middle of the range of interest.

Unfortunately, in our prototype modem the reference levels used to compute the soft decision are affected by a noticeable ripple. This impairment does not appreciably degrade the BER performance of the modem and the Viterbi decoder, but it does affect the characteristics of our signal quality estimator by raising the estimation error considerably. We designed and applied a conceptually simple method in order to overcome this deficiency of our modem. The method is of general validity and we recommend its usage for any practical application. It consists of measuring the probabilities $P_i(R)$ for each quantisation level by using the modem in intermediate frequency (140 MHz) loop-back with AWGN and then using these probabilities instead of the theoretical ones given by (1) to obtain the optimum weights q_i.

An analytical model for the quality estimator using a modem impaired as described above is described in Appendix II.

The characteristics of the signal quality estimators are depicted in Fig. 4. As previously described, the means are invertible functions of E_b/N_o, which makes them usable as E_b/N_o estimators. The variances can be viewed as figures of merit because a low variance implies a high estimation accuracy; the variances are relative to the estimated E_b/N_o value in dB, so their measuring unit is dB². The theoretical variance $\sigma_q^2(R)$ obtained using (1) is much lower than the experimentally measured variance for all values of E_b/N_o and also has a different shape. The reason for this difference is well understood, and in fact the analytical model accounting for the residual ripple of our modem is an excellent fit for the values measured. Both the real estimator with which we made the measures and the analytical model use weights q_i, optimised in terms of their respective characteristics.

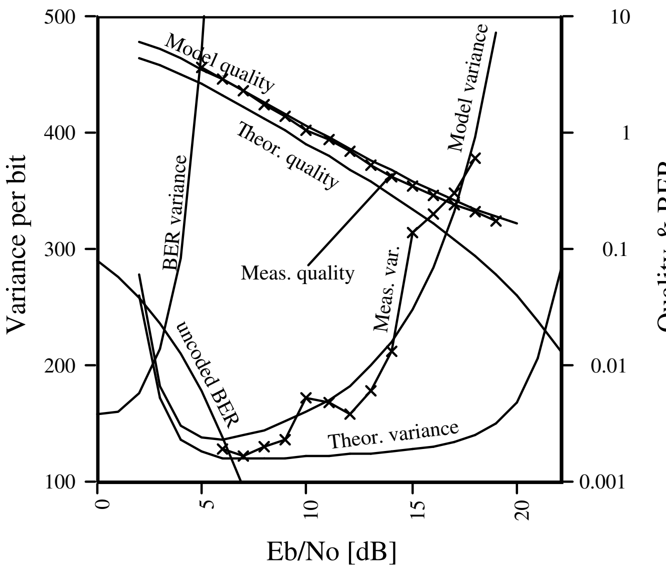

Fig 4. Mean value (arbitrary units) and variance of the signal quality estimator versus the channel Eb/No. "Theor." is the theoretical case, "Model" is the analytical model of our modem, "Meas." are the experimentally measured values

The mean values $\mu_q(R)$ are shown for the theoretical case, the model case and the experimental measures. For this quantity too, the match between the model and the measures is excellent.

The curve labelled "BER variance" shows the variance of the estimation of E_b/N_o obtained using an estimator based on the Viterbi decoder recovered errors rather than on soft decisions [5]. The superior performance of the quality estimator described in this section is clear especially for high E_b/N_o, i.e., for high quality channels where the variance of the quality estimator is much lower.

III. SIGNAL DEGRADATION ESTIMATION

The total degradation of the signal (up-link plus down-link) is obtained by estimating the E_b/N_o ratio available at the station receiver. However, a station must separately estimate the up-link attenuation in order to compensate for it using up-power control. In fact, a station must keep a power level at the satellite transponder input equal to the RB's level which is assumed as a reference power level.

As data is sent at a certain time after the last estimation of the signal quality, the signal degradation needs to be predicted in order to use the most suitable data transmission parameters. Hereafter *attenuation* will be used to mean the signal attenuation measured on the up-link or down-link signal paths, which is the sum of *bulk attenuation* plus *scintillation* [19]; the latter accounts for short term variations. Following the scintillation model described in [1], we assume that the future attenuation has a mean value equal to the current value for a range of a few seconds [14]. The time dependent variance obtained from the same model is used as the basis for computing a suitable margin that is added to the mean value. The evaluation of this margin and the strategies to minimise it are the subject of the rest of the paper.

Let us assume that each transmitting station can estimate its own up-link attenuation and the E_b/N_o at its own receiving input. Here is how these estimates are used to compute the correct up-power control, bit rate and FEC rate to be used when transmitting to a given station. Each station estimates its own down-link degradation by measuring the E_b/N_o at its receiving input with reference to the nominal condition, i.e., when the power level of its own transmission at the satellite transponder is the same as the master RB's power level. All stations broadcast their estimates. Additionally, each transmitting station evaluates for itself the total degradation of the link to a given receiving station by composing the down-link degradation level of the receiving station and the contribution due to its own up-link degradation. This second term is null when the up-link power control is sufficient to compensate for the whole up-link attenuation. The total degradation level is augmented with a suitable margin computed with reference to the future time when the data will be transmitted on the link. The resulting estimate is used to compute the FEC coding and bit rate needed to ensure the BER performance required by the user [2].

Hereafter a denotes the attenuation and r the E_b/N_o ratio. The sub-scripts u and d refer to up-link and down-link parameters, respectively. When a capital letter is used, the above quantities are expressed in dB. For example, for the down-link attenuation we have: $A_d = 10 \text{ Log}_{10}\, a_d$.

According to the fractional Brownian motion [17] model proposed in [1] for the scintillation process, a difference process $W(t_1, t_2) = A(t_1) - A(t_2)$ can be defined which only depends on the difference $t = t_2 - t_1$ for t below a few seconds, so it can be written as $W(t)$. The process $W(t)$ can be considered Gaussian with dB variance σ_W^2, which is a function of the bulk attenuation A_b (expressed in dB) and of the time interval t. Although the model defines a dependence of σ_W^2 on the bulk attenuation, we found that in practice the total attenuation (bulk attenuation plus scintillation) can be considered instead, because the resulting error is negligible. Consequently, in the following we will consider σ_W^2 as a function of the total attenuation A and the time interval t. This model is suitable for predicting the attenuation variance for t up to 3 or 4 s using the relation

$$\sigma_W^2 = V(A)\, t^{2H(A)}. \tag{4}$$

Let us now look at the effects produced by both the down- and up-link attenuations on the signal degradation uncertainty. We define r_{d_c} and r_{u_c} as the down- and up-link E_b/N_o in clear sky conditions, respectively. First we deal with the E_b/N_o estimated by the receiving station. Denoting by r the E_b/N_o at the receiving station input, we have the approximate relation

$$r = \frac{r_u r_d}{r_u + r_d}. \tag{5}$$

Neglecting the variation of the equivalent noise temperature with a_d, we have that $r_d = r_{d_c} / a_d$. Let r_r be the reference E_b/N_o at the station input, i.e. the value of r when the reference power level is received by the satellite. We have

$$r_r = \frac{r_{u_c} r_{d_c}}{a_d r_{u_c} + r_{d_c}}. \tag{6}$$

Let the process $W_r(A_d, t)$ be the difference at the receiving station input between two values of E_b/N_o at two time instants whose difference is t — for t not longer than a few seconds — when the reference power level is received at the satellite transponder and the down-link attenuation is A_d. We have to evaluate the dB variance $\sigma^2_{W_r}(R_r, t)$ of the process W_r as a function of the reference E_b/N_o and the time difference t.

We limit our analysis to the linear case, i.e. we suppose that the amplitude of the down-link scintillation difference process W_d is small enough to justify the relation

$$W_r = W_d \frac{dR_r}{dA_d}. \tag{7}$$

Assuming that dR_r/dA_d is constant within sufficiently small intervals of A_d, the distribution of W_r can be assumed to be Gaussian, like the distribution of W_d, with a variance given by [7]

$$\sigma^2_{W_r}(R_r, t) = \sigma^2_{W_d}(R_r, t)\left[\frac{dR_r}{dA_d}\right]^2. \tag{8}$$

Let us now examine the effect of the up-link attenuation on r. Due to the multicarrier access to the transponder, the satellite high power amplifier (HPA) must operate within the linear zone, without automatic gain control (AGC). We can thus consider the satellite transponder as a linear device, and hence we have

$$r_u = \frac{r_{u_c}}{a_{u_r}} \quad \text{and} \quad r_d = \frac{r_{d_c}}{a_{u_r} a_d}$$

where a_{u_r} is the residual up-link attenuation after up-power control, i.e.

$$A_{u_r} = \max[0, (A_u - A_{p_r})],$$

where $[0,\ A_{p_r}]$ is the up-power control range. From (5) and (6) we get

$$R = R_r - A_{u_r}, \tag{9}$$

i.e. the dB contribution of the residual up-link attenuation can be simply subtracted from the reference E_b/N_o to get the resulting E_b/N_o available at the receiving station input.

We can now evaluate the variance of the attenuation prediction at a future time t. We use the last estimation $\hat{x}$ of the attenuation process as a prediction. Its variance $\sigma^2_{\hat{x}}$, estimated for the instant t, is propagated to the instant $t + \tau$ in which data, sent with the transmission parameters chosen according to $\hat{x}$, are received. Assuming that the estimation error and the scintillation process evolution are independent,

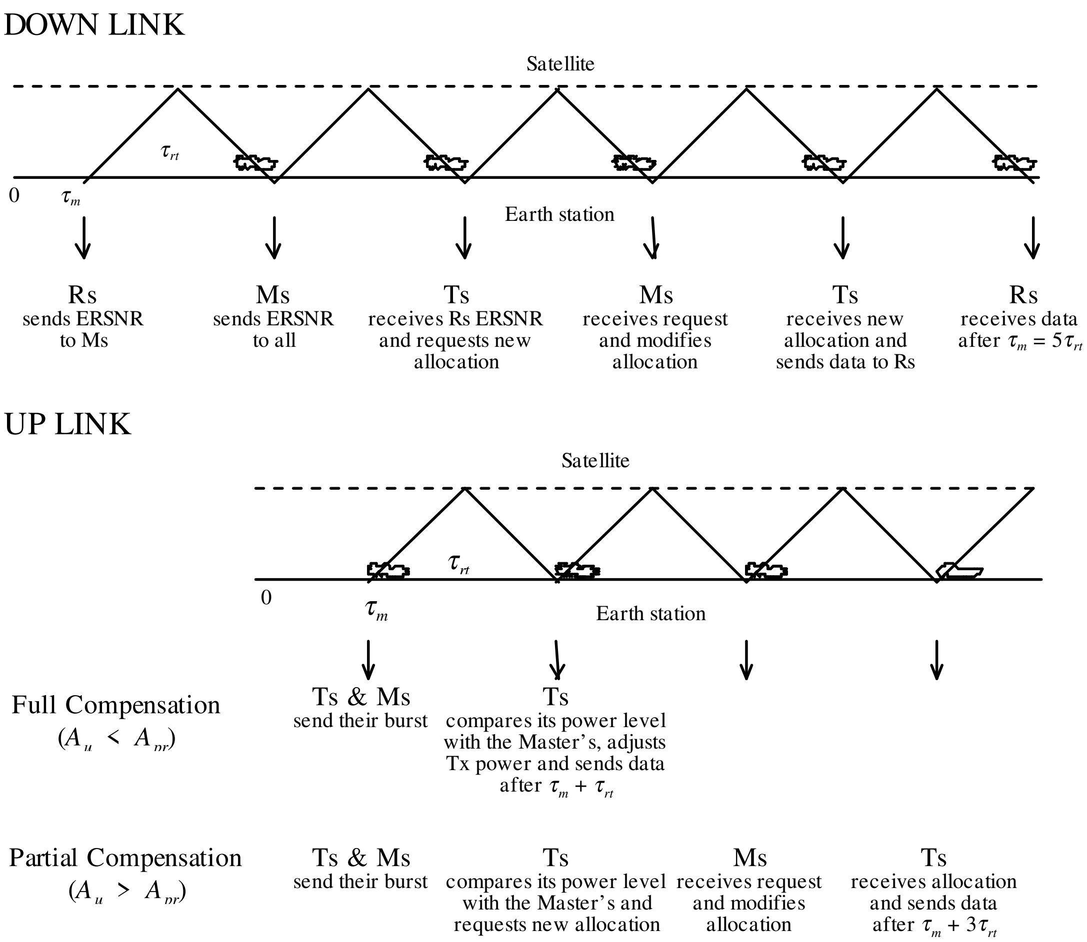

Fig 5. Temporal scheme for estimating up-link attenuation and reference E_b/N_o (down-link). Legend: Ms: master station, Rs: receiving station, Ts: transmitting station, ERSNR: Estimated Reference Signal to Noise Ratio (E_b/N_o), τ_m: measurement time, τ_{rt}: round trip time

the propagated variance of either A_u or R_r is

$$\sigma_x^2 = \sigma_{\hat{x}}^2 + \sigma_\tau^2 \tag{10}$$

where σ_τ^2 is given by (4) with $t = \tau$ when the process A_u is considered, and by (8) after substituting the variance given by (4) when the process R_r is considered.

The process R_r is evaluated using the soft level quality estimator, while A_u can be estimated by measuring the power level of the signal received using a narrow-band carrier envelope estimator. Most of the hardware required for such a device is already in place in a modem that includes a fast AGC for building the data reference level. We assume that the demodulated signal is low-pass filtered, squared and converted into dB using a look-up table. After elaborating the signal this way, the dB variance of each sample is

$$\sigma_s^2 = (10\log_{10} e)^2 \frac{2}{r\,\alpha_b} \tag{11}$$

where α_b is the ratio between the bandwidths of the signal and the low-pass filter.

Each traffic station broadcasts its R_r estimate to all the other stations. The transmitting station estimates its own A_u and computes R at the receiving station using relation (9). Then it decreases R by a margin value M, which depends on the variance of the R estimation which we denote by σ_R^2.

The value of σ_R^2 is estimated by summing the variances of the up-link estimation of the transmitting station and the down-link estimation of the receiving one. Indeed, since scintillation is a local phenomenon mainly attributed to tropospheric turbulence [19], the most reasonable assumption is a complete uncorrelation between processes W_u and W_r since the two processes are related to scintillation at different geographical locations.

Finally, the resulting R is used to choose the appropriate FEC coding and bit rates of the data to transmit according to the BER required.

IV. OPTIMISING THE MEASUREMENT TIME

Both the variances on the right hand side of (10) depend on the measurement time interval which we denote by τ_m. The measurement error decreases while the variance of the scintillation process increases with an increasing measurement time, so the derivatives of $\sigma_{\hat{x}}^2$ and σ_τ^2 with respect to τ_m have opposite signs. It turns out that their sum σ_x^2 can be minimised, which we do for both down and up sides separately. Fig. 5 shows the temporal schemes for estimating the reference E_b/N_o and the up-link attenuation. While in the up-link case we have to estimate the attenuation variance at the future data transmission time, in the down-link case the estimation has to be made for the moment when data are received.

A. Down-link Case

The predicted variance of R_r can be expressed, using (10), as

$$\tilde{\sigma}^2_{R_r} = \sigma^2_m(R_r, b_r, \tau_m) + \sigma^2_{W_r}(R_r, \tau_d + \tau_m/2)\,, \quad (12)$$

$$where\ \sigma^2_m = \frac{\sigma^2_{\hat{R}}(R_r)}{b_r\tau_m},$$

$\sigma^2_{\hat{R}}$ is the bit quality variance shown in Fig. 4, b_r is the average bit rate of the bit sequence employed for the estimation, that is, the reference burst, $\sigma^2_{W_r}$ is taken from (8) and τ_d is the delay between the estimation of R_r and the reception of data with coding and bit rates based on that estimation. We take at least one sample per frame, assuming that τ_m is many frames long, and that the estimation of R_r is recomputed once per frame by taking the moving average of samples over the interval τ_m. Then, each estimation can be considered as referring to a time $\tau_m/2$ in the past, and the delay between measuring and data reception is $\tau_d + \tau_m/2$.

B. Up-link Case

A_u is estimated by the traffic stations by comparing the RB power level received with the power level received of their own bursts. The RB always has the nominal power level at the satellite input because we assume that the master never experiences severe fading, so that its up-power reserve is enough to compensate for any up-link attenuation. Whenever the current master detects an excessive fade level, its role is taken by another station. In each traffic station we have $A_u = \Delta P_{cT} + A_{u_r}$, where ΔP_{cT} is the difference in dB between the station transmission power needed in clear sky conditions and the power currently transmitted as a best effort to track the RB level; A_{u_r} is the residual up-link attenuation.

In the case of the master station, $A_u + A_d$ can be evaluated as $\Delta P_{cT} + \Delta P_{cR}$, where ΔP_{cR} is the difference between the power level of the RB currently received and the nominal level for clear sky conditions. In order to estimate A_u alone, the master uses a beacon receiver to measure A_d. The beacon receiver operates in continuous mode, so its bandwidth can be made narrower than the one of the signal level estimator which operates on actual data in burst mode.

Relation (11) is also applicable to samples of the beacon receiver output.

The predicted variance of A_u, as estimated by the master using (10), is

$$\tilde{\sigma}^2_{MM} = \sigma^2_{s_M}(R_r, n_{s_M}) + \sigma^2_{A_u}(A_u, \tau_{rt} + \tau_{m_M}/2)\,, \quad (13)$$

where τ_{m_M} is the measurement time interval of the master,

$$\sigma^2_{s_M} = [\sigma^2_{sl}(R_r) + \sigma^2_{bl}(R_r)]/n_{s_M}$$

where σ_{sl}^2 and σ_{bl}^2 are the variances of the signal and the beacon level estimators, respectively and n_{s_M} is the number of samples (one per frame) in the measurement interval time of both the signal and the beacon levels. The second addendum on the right hand side of (13) is the variance contributed by the attenuation process evolution, given by (4), between the measurement and the up-link power adjustment time made by the master. We take one sample per frame, assuming that the estimation of $\tilde{\sigma}^2_{MM}$ is computed once per TDMA frame by taking the moving average of samples over the interval τ_{m_M}. Then the estimation refers to a time $\tau_{m_M}/2$ earlier in the past. The term τ_{rt}, which is the satellite round trip time, is added because the data received have experienced an up-link attenuation at a time τ_{rt} earlier.

As far as the variance of the A_u prediction made by the traffic stations is concerned, from (10) we obtain

$$\tilde{\sigma}^2_{A_u} = \tilde{\sigma}^2_{MM} + \sigma^2_{s_T}(R_r, R, n_{s_T}) + \sigma^2_{A_u}(A_u, \tau_u + \tau_{m_T}/2)\,, \quad (14)$$

where

$$\sigma^2_{s_T} = [\sigma^2_{MT}(R_r) + \sigma^2_{TT}(R)]/n_{s_T}\,,$$

where σ_{MT}^2 and σ_{TT}^2 are the variances of the signal level estimated by the traffic station when the master reference burst or its own burst is received, respectively and n_{s_T} is the number of samples (one per frame) taken in the measurement time interval τ_{m_T}. The last addendum of (14) is the process evolution given by (4), where τ_u is the delay between the estimation of A_u and the data reception time.

V. RESULTS

Table I reports the values of the parameters used, most of which were chosen because they are the ones implemented in our experimental modem.

The reference E_b/N_o ratio, equal to 12 dB in clear sky

PARAMETER NAME	VALUE
$R_{u_c} = R_{d_c}$ (clear sky E_b/N_o)	21 dB
Ref. burst E_b/N_o in clear sky	18 dB
Traffic burst E_b/N_o	12dB max(clear sky), 6dB min
frame length	20 ms
Reference burst bit rate	2 Mbit/s
Reference burst length	1000 bit
b_r (average RB data rate)	50 Kbit/s
data bit rate	variable: 8, 4, 2, 1 Mbit/s
data coding rate	variable: 1/2, 2/3, 4/5, 1
τ_{rt} (round trip time)	250 ms
τ_d	1,250 ms ($5\tau_{rt}$)
τ_u (full A_u compensation)	250 ms (τ_{rt})
τ_u (partial A_u compensation)	750 ms ($3\tau_{rt}$)
α_b (data pow. lev. filter)	64
α_b (beacon pow. lev. filter)	512

Table I. Numerical values of the parameters conditions, gives a BER of 10^{-8} with uncoded data. This BER can be maintained for E_b/N_o dropping down to 6 dB by using lower FEC coding rates, and the gain in reducing the data rate from 8 to 1 Mbit/s is 9 dB. Thus the gain in the FEC coding plus bit rate variations is 15 dB, which added to 10 dB of up-power control range gives a total 25 dB operating range for the fade countermeasures considered. This means that the up-link degradation of the sending station plus the down-link degradation of the receiving station cannot exceed 25 dB. The bit rate of the reference burst is 2 Mbs, which gives an E_b/N_o of 18 dB in clear sky. Since, due to the burst preamble acquisition performance of our experimental modem, we did not use E_b/N_o values lower than 6 dB, in the following we considered a maximum down-link degradation of 12 dB.

In order to simplify the presentation of the numerical results, we did not account for the up-link and down-link attenuations separately in the computation of R_r, which would have required many results to be expressed as functions of two variables. We decided to use a single independent variable instead, with the assumption that

$$A_d = 0.5\, A_u, \tag{15}$$

with reference to the same station using the long-term frequency scaling formula given in [11]. Therefore, the variance of the down-link estimation R_r is expressed as a function of a single variable, while a real system using this fade countermeasure policy would use the exact computation instead. In the following, we will comment on the error introduced by this assumption on our numerical results.

We used the values for $V(A_u)$, $V(A_d)$, and $H(A_u)$, $H(A_d)$ obtained in [1]. Corrections to apply for different frequencies, elevation angles and dish diameters can be found in [16], while [18] gives information about the dependence of scintillation on season and other factors in clear air conditions.

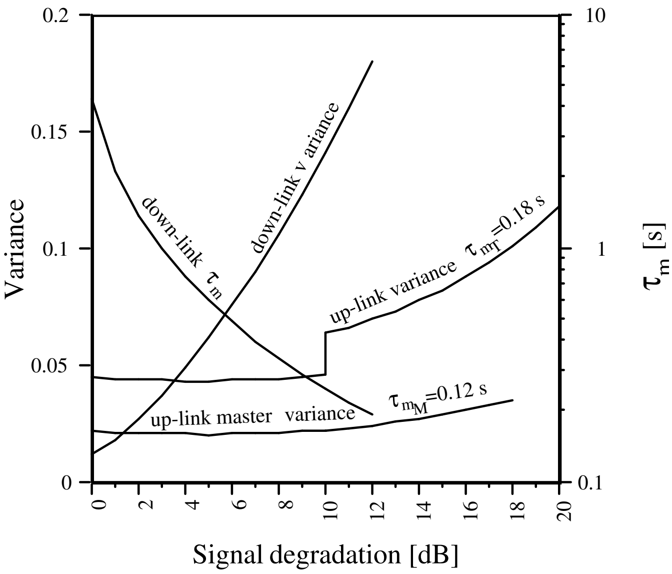

Fig 6. Variances of the signal degradation on the down-link (R_r) and on the up-link (A_u) versus R_r degradation and A_u, respectively. The optimum measurement times and the master up-link attenuation variance are shown as well

A. Predicted Variances

The variance $\tilde{\sigma}^2_{R_r}$ of the down-link estimation R_r is plotted in Fig. 6 versus the R_r degradation. The R_r degradation is intended as the difference from the reference (clear sky) condition. $\tilde{\sigma}^2_{R_r}$ is obtained by minimising relation (12) with respect to τ_m for all values of the R_r degradation. The resulting optimum value of τ_m is also plotted in Fig. 6. The quality estimation variance $\sigma_q^2(R)$ used for the evaluation of $\tilde{\sigma}^2_{R_r}$ is computed according to the analytical model that is mentioned in Section II. A plot of $\sigma_q^2(R)$ is shown in Fig. 4 under the label "*Model variance*". Choosing the theoretical variance instead with the weights optimised for the quality defined in (1) would not produce any appreciable improvements. In fact, the contribution of the quality estimator to the total estimation error is less than 10%.

The variance of the master reference level $\tilde{\sigma}^2_{MM}$ is obtained by minimising (13), and it is plotted in Fig. 6 versus the up-link attenuation of the master station. The optimum measurement time τ_{m_M} is only slightly dependent on the up-link attenuation, so a constant value was assumed, equal to 0.12 s. Also, $\tilde{\sigma}^2_{MM}$ does not vary significantly for attenuations below the full up-link compensation limit (10 dB) where we suppose that the master operates, so hereafter we assume that it is constant and equal to its value at 10 dB.

The variance $\tilde{\sigma}^2_{A_u}$, as computed by each traffic station, is then obtained by minimising relation (14) after substituting (15), and is plotted in Fig. 6 versus A_u itself. As for the master reference level, the optimum measurement time interval τ_{m_T} has a very small variation range, so hereafter we assume the constant value of 0.18 s.

B Power Margins

Assuming uncorrelation between processes W_u and W_r, we have

$$\sigma^2_R = \tilde{\sigma}^2_{R_r} + \tilde{\sigma}^2_{A_u}\,. \tag{16}$$

Denoting by p_e the probability of error, we assume that we know the relation $p_e(R)$ at the data decoder for each type of FEC coding. The average p_e for a given value $\overline{R}$ of the channel E_b/N_o, which is estimated with a variance $\sigma^2_{\overline{R}}$ given by (16), is

$$p_e(\overline{R}) = \int_{-\infty}^{+\infty} p_e(R)\frac{1}{\sqrt{2\pi}\,\sigma_{\overline{R}}} e^{-\frac{(R-\overline{R})^2}{2\sigma^2_{\overline{R}}}}\, dR\,. \tag{17}$$

Substituting p_e given by (17) in the inverse function of $p_e(R)$, we get the equivalent value $R_e\big(p_e(\overline{R})\big)$. The margin to be applied on the estimated value $\overline{R}$ is then

$$M(R) = \overline{R} - R_e\,. \tag{18}$$

We have considered the cases of no FEC coding and 1/2 convolutional coding. Intermediate punctured coding rates of 4/5 and 2/3 give results very close to the 1/2 coded case. For the uncoded case we have [20]

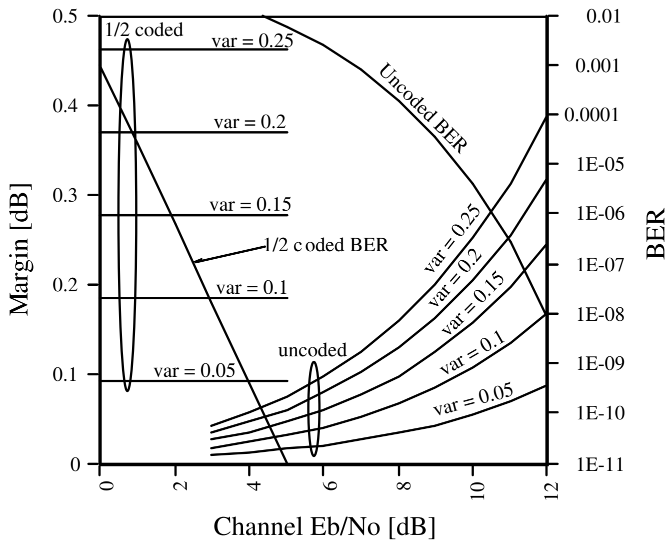

Fig 7. Margin to take into account over the estimation of the total signal degradation and BER versus channel E_b/N_o. Uncoded and 1/2 coded cases

$$p_e = \frac{1}{2}\operatorname{erfc}\left(10^{R/20}\right). \tag{19}$$

For the 1/2 coded case, by interpolating the decoder results [2], we obtain a very good fit using the approximating function

$$p_e = 10^{-(1.6R+3)}, \tag{20}$$

which is linear in logarithmic scale. Since M increases with the absolute value of the derivative of the function $p_e(R)$, the margin does not depend on R in the 1/2 coded case where this derivative is constant.

In Fig. 7 the margin M is plotted as a function of the channel E_b/N_o R for both the uncoded and the 1/2 coded cases, using (17), (18), (19) and (20). The function $p_e(R)$ for both cases is shown as well.

In the case of clear sky, the channel E_b/N_o is the reference one, that is 12 dB; we assume data with no FEC applied (uncoded) are being sent. In this case, the margins M for different values of the variance σ_R^2 are plotted in Fig. 7 versus R, forming a family of concave curves. The variance σ_R^2 to use is obtained from (16), and depends on the up- and down-link degradations. Since we assume clear sky (unfaded) conditions corresponding to a null signal degradation, from Fig. 6 we get a variance of 0.015 for the down-link and 0.045 for the up-link which, using (16), give a total value for σ^2_R equal to 0.06 dB^2. The corresponding curve for the uncoded case in Fig. 7 gives a margin of 0.1 dB for E_b/N_o equal to 12 dB.

At the other extreme, we consider the case of the maximum value of total degradation which can be compensated for by the system, i.e. $A_u + A_d = 25$ dB, where A_u is relative to the sending station, while A_d is relative to the receiving station. Since A_d cannot be greater than 12 dB and the A_d estimation error is prevalent with respect to A_u in (9) (See Fig. 6), the worst case is for a down-link degradation of 12 dB and an up-link degradation of 13 dB. From Fig. 6, we have a variance of 0.18 for the down-link degradation and 0.07 for the up-link degradation for a total variance 0.25 dB^2 for the estimation of the channel E_b/N_o. In such a deep fade condition, we would use a 1/2 FEC coding rate, thus obtaining a margin of about 0.5 dB.

The assumption (15) introduces a negligible error in the margins estimated above. In fact, using (15) is equivalent to introducing an error in the evaluation of R_r [22]. Taking as an example a difference of 3 dB on the down-link attenuation with respect to (15), we obtain (see Fig. 6) an error of 0.03 in the R_r variance, and consequently (see Fig. 7) an error less than 0.06 dB when evaluating the necessary power margin. It should be noted that this is important only when considering a fixed margin; no error is introduced when the system dynamically evaluates the necessary margin because in this case (15) is not used.

If a margin that is variable with the channel degradation is applied, the average margin turns out to be close to the minimum value of 0.1 dB, because most of the time the system works in almost unfaded conditions. On the other hand, a gross value of 0.5 dB can be applied in any conditions thus simplifying the procedure. This value is much lower than in any other system proposed, for example the one described in [9].

In all the cases considered, the second error term in (10), that is, the uncertainty on the evolution of the scintillation process, is much greater than the error produced by the first error term in (10), that is, the inaccuracy of the attenuation estimators. Optimising the measurement time interval played a major role in reducing the variance of the estimators. As a proof of the consequences of this observation, we used a Kalman filter to estimate the attenuations. The result was a reduction in the required margin M by less than a tenth of dB, which is negligible for all practical purposes.

This is the reason why the cost of more sophisticated methods for reducing the accuracy in the estimation of the reference E_b/N_o (such as those proposed in [6, 15]) is not justified by improvements in performance.

VI. CONCLUSIONS

We have described the concept and the implementation details of a complete fade countermeasure system. We have discussed the performance of the system when applied to a centralised control TDMA access scheme, based on demand assignment of capacity allocation. Numerical results are obtained based on the characterisation of the scintillation process in the Ka band described in [1], and on the performance measured of the estimators built in our experimental modem. The value of the margin to take into account in the signal degradation prediction is small in all the cases considered. An accurate dynamic value of the margin can be computed from the estimated attenuation, thus obtaining an average margin in the order of 0.1 dB. Alternatively, a fixed margin of 0.5 dB can be used for total channel attenuations up to 25 dB, assuming an up-power control range of 10 dB.

The margin accounts for two terms, namely the error in estimating the attenuation and the error in predicting the evolution of the scintillation process. Our results indicate that the latter term is largely dominant, which means that more sophisticated methods for estimating the reference E_b/N_o [15] and the up-link attenuation would not significantly reduce the power margin. This would be no longer true if a more precise characterisation of the scintillation process than that described in [1] were available, or if a low-orbit (LEO) system were considered where the signal delays involved, and consequently the variance of the scintillation process, would be much lower.

APPENDIX I: LIST OF SYMBOLS

y_i, b_i	digital datum at the A/D converter, soft decision threshold
E_b, N_o, r, R	energy per bit, one-sided noise power density, E_b/N_o value, E_b/N_o value in dB
$P_i(R)$, q_i	probability of a soft decision quantization level i, weight of a quantization level
q, $\mu_q(R)$	random variable associated with quantization levels (*quality*), and its mean
N, $\overline{q}$	number of received bits, sample mean of quality
$\hat{R}(\overline{q})$, $\sigma^2_{\hat{R}}(R)$	estimated value of R based on $\overline{q}$ (*quality estimator*), and its variance
a, A, a_d, a_u	attenuation value, attenuation value in dB, down-link and up-link attenuations
$W(t)$, σ_W^2	scintillation difference process, and its dB variance
r_{d_c}, r_{u_c}	down- and up-link E_b/N_o in clear sky conditions
r_r, R_r	reference E_b/N_o at the station input (the value of r when the reference power level is received by the satellite), same value in dB
r_u, r_d, r_{u_c}, r_{d_c}	E_b/N_o on the up- and down- links, the same for clear sky conditions
W_r, $\sigma^2_{W_r}$	scintillation difference for the r_r process and its dB variance
W_d, σ^2_{Wd}	down-link scintillation difference and its dB variance
a_{u_r}, A_{p_r}	residual up-link attenuation after up-power control, up-power control range (dB)
$\hat{x}$, $\sigma^2_{\hat{x}}$, σ_τ^2	last estimation of the attenuation process (used as prediction), its variance, and the variance due to the propagation of the estimation to time τ
σ_s^2, α_b	dB variance of a sample of AGC output, ratio between the signal's and the AGC low-pass filter's bandwidths
σ_R^2, τ_m	dB variance of the estimation of R, measurement time interval
$\tilde{\sigma}^2_{R_r}$, τ_d, b_r	predicted variance of R_r, delay from estimation of R_r to reception of data with coding based on that estimation, rate of bit stream employed for the estimation
A_{u_r}, ΔP_{cT}	residual up-link attenuation, transmitted power minus transmission power in clear sky conditions (dB)
ΔP_{cR}	nominal received RB level in clear sky conditions minus received RB level (dB)
$\tilde{\sigma}^2_{MM}$, τ_{m_M}	variance of A_u predicted by the master, measurement time interval of the master
$\tilde{\sigma}^2_{A_u}$, τ_{m_T}	variance of A_u predicted by traffic stations, and their measurement time interval
τ_{rt}, τ_u	satellite round trip time, delay from estimation of A_u to data reception time
$p_e(R)$, $M(R)$	bit error probability, margin to apply to the estimated R versus R itself

APPENDIX II: QUALITY ESTIMATOR FOR THE EXPERIMENTAL MODEM

The model takes into account the ripple that affects the reference level of the demodulated data of our experimental modem. It consists of superimposing a sinusoidal wave over the reference level whose frequency is much lower than the bit rate. The probabilities of the various quantisation levels $P_i^{(j)}$ are then obtained by averaging over one observation interval.

From (1) we have

$$P_i^{(j)}(R) = \frac{1}{2T_m}\int_0^{T_m}\left\{\begin{array}{l}\mathrm{erfc}\left[10^{R/20}(r_l - h_i)\right] - \mathrm{erfc}\left[10^{R/20}(r_l - h_{i-1})\right] \\ + \mathrm{erfc}\left[10^{R/20}(r_l + h_{i-1})\right] - \mathrm{erfc}\left[10^{R/20}(r_l + h_i)\right]\end{array}\right\} dt,$$

where $r_l = 1 + k sin(\frac{2\pi\gamma}{T_m}t + \varphi)$,

T_m is the measurement time interval in which N bits are considered, γ is the number of cycles in the interval T_m and k is the amplitude of the sinuisodal wave. The integral in the above equation is independent of φ if γ is an integer or $\gamma \gg 1$, i.e. if T_m is an integer number of cycles long or is long enough to make the contribution of the last fraction of the cycle negligible. The latter is our case, so we can assume $\varphi = 0$ and $\gamma = 1$ without significantly affecting the result. We then made the calibration of the coefficient k by equating the mean value of the quality

$$\mu_q^{(j)}(R) = \sum_1^{Q/2} q_i P_i^{(j)}(R)$$

to the measured value at 10 dB. The resulting value of k was 0.12.

ACKNOWLEDGEMENTS

The authors wish to thank Dr. Mario Mauri of CSTS (Centro Studi sulle Telecomunicazioni Spaziali) Institute for providing the attenuation data, Dr. Erina Ferro of CNUCE for fruitful discussions, encouragement and ideas and Dr. Santi T. Rizzo for programming and computations as a collaborator of CNUCE.

REFERENCES

[1] N. Celandroni, F. Potortì "Modeling Ka band scintillation as a fractal process," *IEEE J. Select. Areas Commun.*, Vol.17 No.2, February 1999.
[2] N. Celandroni, E. Ferro, N. James and F. Potortì, "FODA/IBEA: a flexible fade countermeasure system in user oriented networks," *Intern. Journal of Satellite Communications,* Vol.10 No.6, pp.309-323, 1992.
[3] N. Celandroni, E. Ferro and F. Potortì, "The performance the FODA/IBEA satellite access scheme measured on the Italsat satellite," *Proc. of the ICDSC-10 Conference V.1*, Brighton (US), pp.332-338, May 1995.
[4] N. Celandroni, E. Ferro, F. Potortì, A. Bellini and F. Pirri, "Practical experiences in interconnecting LANs via satellite," *ACG SIGCOMM Computer Communication Review,* Vol.25 No.5, pp.56-68, October 1995.
[5] N. Celandroni and S. T. Rizzo, "Detection of Errors Recovered by Decoders for Signal Quality Estimation on Rain Faded AWGN Satellite Channels", *IEEE Trans. on Communications,* Vol.46 No.4, pp.446-449, April 1998.
[6] N. Celandroni, E. Ferro and F. Potortì, "Quality estimation of PSK modulated signals", *IEEE Communications magazine*, July 1997.
[7] A. Papoulis, *Probability, Random Variables and Stochastic Processes,* McGraw-Hill, 1991
[8] Y. Yasuda, Y. Hirata and A. Ogawa, "Optimum Soft Decision for Viterbi Decoding," *IEEE 5th International Conference on Satellite Communications*, Genova (IT), 1981.
[9] H. Kazama, T. Atsugi, M. Umehira and S. Kato, "A Feedback-Loop Type Transmission Power Control for Low Speed TDMA Satellite Communication Systems," *Proc. IEEE ICC*, Boston (US), 1989.
[10] E. Russo, "Implementation of a space diversity system for Ka-band satellite communications", *IEEE ICC*, 1993.
[11] *CCIR Report 564-4*, "Propagation data and prediction methods required for earth-space telecommunications systems", 1990.
[12] L. Dossi, G. Tartara and E. Matricciani, "Frequency diversity in millimeter wave satellite communications, "*IEEE Trans. on Aerospace and Electronic Systems*, Vol.28, No.2, April 1992.
[13] F. Carassa, E. Matricciani and G. Tartara, "Frequency diversity and its applications," *International Journal of Satellite Communications*, Vol.6, pp.313-322, 1988.
[14] L. Dossi E. Matricciani and M. Mauri, "Robust control system for resource-shared satellite networks affected by rain attenuation" *Alta Frequenza*, Vol.6 No.6, November-December 1994.
[15] D. Kreuer and E.Bierbaum "Improved Eb/No Estimation with Soft Quantized Detection," *Proc.* of *PIMRC'94/WCN*, Den Haag (NL), Sept. 1994, pp.620-624.
[16] Vilar, Filip, "Measurements of 20-30 Ghz amplitude scintillations. Dependence of the statistics upon the ground station measuring parameters", *Proc. Olympus Utilization Conf.*, Wien, 1989.
[17] H. O. Peitgen, and D. Saupe, "The science of fractals images", Springer-Verlag, New York (US) 1988.
[18] G. Peeters, F. S. Marzano, G. D'Auria, C. Riva, D. Vanhoenacker-Janvier, "Evaluation of statistical models for clear-air scintillation prediction using Olympus satellite measurements", *Int. J. Satellite Comm.*, Vol.15, 1997, pp.73-88.
[19] E. Matricciani, M. Mauri, C. Riva, "Relationship between scintillation and rain attenuation at 19.77 GHz", Radio Science, Vol.31, No.2, pp.273-279, March-April 1996.
[20] J. G. Proakis, *Digital Communications.* McGraw-Hill, 1995.
[21] F. Carassa, "Adaptive methods to counteract rain attenuation effects in the 20/30 Ghz band", *Space Communication and broadcasting*, Vol.2 No.3, September 1984
[22] Y. Otsu, Y. Furuhama, S. Hoshina, S. Ito, "Propagation measurements and TV-reception tests with the Japanese broadcasting satellite for experimental purposes", *IEEE transactions on Broadcasting*, Vol.BC-25 No.4, pp.113-120 September 1979

Nedo Celandroni received his Dr. Ing. degree in Electronic Engineering from the University of Pisa, Italy, in 1973. Since 1976 he has been a researcher with the CNUCE Institute of the Italian National Research Council (C.N.R.). He worked for the realization of the Flight Dynamic System of the SIRIO satellite. Since 1979 he has been involved in the field of digital satellite communications. He partecipated to several projects in this field: STELLA I/II (Satellite Transmission Experiment Linking Laboratories), FODA (Fifo Ordered Demand Assignment), FODA/IBEA (Information Bit Energy Adaptive), Progetto Finalizzato Telecomunicazioni, Experiments on the satellites Olympus and Italsat. His interest includes rain fade countermeasure systems, data quality estimation, VSAT systems, and GEO MEO and LEO orbits satellite for mobile telephony and multimedia systems.

Francesco Potortì received his Electronic Engineering degree from the University of Pisa, Italy, in 1991. He is currently a full-time researcher at the CNUCE-CNR Institute in Pisa, Italy, where he has worked since 1989 as a member of the Computer Network group, in the fields of satellite communication protocols and fade countermeasure systems. His main research interests include communications protocols and their implementation, LEO satellites, Internet technology with regard to integrated services and TCP, simulation of communications systems. Since 1997 he has taught at the Engineering Faculty of the University of Pisa.